SI Appendix

Experimental design

I. TASK.

Participants performed a simplified “coffee-tea making” task adapted for functional magnetic resonance imaging (fMRI) from a more complex "activities of daily living" task paradigm (1). Each trial consisted of a sequence of six decision states, each of which was characterized by a 3-item image describing 3 possible action choices, followed by a feedback state (Fig. 2). For each decision state, the subjects were required to select one of the 3 actions by pressing a spatially-corresponding button on a box using their dominant hand. At the end of each trial the subjects were presented with a smiley face for correct performance and a sad face for incorrect performance. Across trials each decision state always entailed selecting between the same 3 actions (for example, State 1 always required a choice between coffee grinds, tea leaves, and pepper), but the positions of the images within each state varied across and within trials (for example, the sugar image appeared equally often on the left, middle, and right locations). Thus the decisions involved selecting between action concepts (for example, whether to select the spoon, fork or knife) rather than the specific actions that implement those decisions (whether to press the left, middle or right buttons).

Subjects were presented with a cover story that they were a barista at a café whose job it was to prepare coffee and tea according to the following set of specialized rules. 1) Across trials, coffee vs. tea must be made at random. Thus, for State 1 the subjects must select either the coffee grinds or tea leaves “as if flipping a coin”. 2) Cream and water can only be added to coffee, and sugar and water can only be added to tea. Thus, for States 2 and 4, the subjects must choose either cream or water when making coffee, or sugar and water when making tea. 3) The first ingredient added to each beverage must be selected at random. Thus, for State 2, the subjects must add either of the two allowable ingredients (cream and water for coffee, and sugar and water for tea) “as if flipping a coin”. 4) The same ingredient cannot be added twice to the same beverage. Thus, for State 4, the subjects must select the complementary ingredient to what was selected in State 2; for example, if they already added water when making tea, then in State 4 they must add sugar. 5) The subjects must “stir” in each ingredient after adding it. Thus, for States 3 and 5, the subjects must always select the spoon. 6) Once the beverage has been prepared, the subject must bring it to the customer. Therefore, for State 6 they must select coffee when making coffee and tea when making tea. Note that the pepper shaker, fork, knife, and orange juice images acted as distractors that the participants were required to ignore. A smiley face was presented at the end of each correctly-executed sequence (signifying a happy customer); otherwise a sad face was presented. Application of the rules resulted in execution of four different task sequences (Fig. 2). Because the image triplets for each step were identical across the four sequences, the task requires subjects to maintain contextual information about their past actions throughout each sequence, namely, whether they are making coffee or tea, and which ingredient they added first. Note further that the combination of 6 stimulus events with 4 allowable action sequences describes a total of 24 different states.

www.pnas.org/cgi/doi/10.1073/pnas.1803650115

The task was coded using MATLAB (Mathworks, Nantucket, MA) and Psychtoolbox, Version 3. Each decision state image (Fig. 2, States 1-6) was shown for 1 s and was followed by a black screen for 2.5-4.5 s (mean 3.5s, with 7 possible jitters at .33 s increments); if the response was not executed during presentation of the state image or during the subsequent black screen, then the words “too slow” appeared and the trial was considered incorrect. The outcome stimulus (i.e., happy or sad face; Fig. 2, State 7) was presented for 1 s. A 3 s interval followed each trial. The screen resolution was 1024 × 768 pixels and each image was 200 × 200 pixels wide.

II. COMPUTATIONAL MODEL.

We utilized an existing RNN model of MCC function (2) to simulate MCC representations during execution of the coffee-tea making task. The model is an Elman network, which is composed of 4 layers of units including an input layer, a hidden layer, a context layer, and an output layer (Fig. 1A). The context layer receives an exact copy of the activation values of the units in the hidden layer on each step of the simulation, and then returns those values to the hidden layer units on the subsequent step, enabling the network to retain information about past states (3). The input layer was comprised of 6 units denoting the action on the current sequence step (add coffee, add tea, add water, add milk, add sugar, stir) and a seventh “start” unit indicating the beginning of the trial (depicted with the letter “S” in Fig. 1A). The output layer was composed of 8 units denoting possible actions to occur on the subsequent sequence step (add coffee, add tea, add water, add milk, add sugar, stir, serve coffee, serve tea). Both the hidden and context layers were composed of 15 units. For each of the four sequences in the coffee-tea task, the network was trained using backpropagation through time to predict each forthcoming action based on the immediately preceding action (3). To be specific, the network was trained on the following sequences:

```
Sequence 1:
State: Input   -> Output
1:     start   -> coffee
2:     coffee  -> milk
3:     milk    -> stir
4:     stir    -> water
5:     water   -> stir
6:     stir    -> serve coffee

Sequence 2:
State: Input   -> Output
1:     start   -> coffee
2:     coffee  -> water
3:     water   -> stir
4:     stir    -> milk
5:     milk    -> stir
6:     stir    -> serve coffee
```

```
Sequence 3:
State: Input   -> Output
1:     start   -> tea
2:     tea     -> sugar
3:     sugar   -> stir
4:     stir    -> water
5:     water   -> stir
6:     stir    -> serve tea

Sequence 4:
State: Input  -> Output
1:     start   -> tea
2:     tea     -> water
3:     water   -> stir
4:     stir    -> sugar
5:     sugar   -> stir
6:     stir    -> serve tea
```

100 networks with random initial weights (normal distribution: mean = 0, standard deviation = 1) were each trained 5000 iterations on the 4 sequences. Sequence presentation was interleaved and determined at random with equal probability. In keeping with (2), the learning rate was set at 0.5, and all the networks performed better than the performance threshold reported therein.

Following training, the network was again presented with the 4 input sequences, and the activation values of the 15 context units were read out from the network for each of the 6 steps of each sequence. These values were then used to determine the predicted 24 × 24 representation dissimilarity matrix as described in the main text.

III. EXPERIMENTAL PROCEDURE.

III. A. Participants. 18 volunteers participated in this experiment (13 females, 5 males; median age 22, range 19-29) for pay (40 Euros; 3 participants earned an extra 10 Euros for overtime). Because the statistical effect sizes for the predicted results were unknown at the time of study design, the sample size was based on the current practice in human fMRI research of about 20 subjects per study. Participants had normal or corrected-to-normal vision and reported being free of neurological or language disorders. The experimental protocol was approved by the Ethical Committee of Ghent University Hospital and by the University of Victoria Human Research Ethics Board. Participants signed an informed-consent form before they began the experiment, and were screened for magnetic materials before entering the scanner room. The experiment was conducted in accordance with the ethical standards prescribed in the 1964 Declaration of Helsinki.

III. B. Task procedure. Before entering the scanner, participants were guided through the task and then practiced it on their own for 6 trials; it was emphasized that they should randomize

the sequence orders “as if flipping a coin”. They then completed 4 blocks of 18 trials in the scanner, for a total of 72 trials, with short, self-paced rest breaks between blocks. At the end of each block of trials, a feedback screen indicated the total numbers of coffees vs. teas prepared on that block. After exiting the scanner, participants responded to a questionnaire that assessed their task strategies (if any), and were then debriefed, paid, and dismissed.

III. C. Magnetic resonance imaging data acquisition. Structural and functional images were acquired using a Siemens 3 T Magnetom Trio MRI scanner equipped with a 32-channel radio-frequency head coil. For each participant, anatomical, T1-weighted structural images were acquired with an MP-RAGE pulse sequence at the beginning of the scanning session. Functional images were acquired with an echo-planar imaging pulse sequence (33 slices per volume, TR=2000 ms, slice thickness = 3 mm, voxel size = 3.0 mm × 3.0 mm × 3.0 mm, FoV=224 mm, flip angle =80°). 320 volumes per run were collected during 4 runs. The first trial in a run started after the first five volumes of each run were acquired during presentation of a black screen; these first five volumes were not used in the analyses.

Data and statistical analyses

I. MRI PRE-PROCESSING AND GENERAL LINEAR model.

I. A. Pre-processing. Processing and statistical analyses of the functional images were conducted using SPM12 software (Wellcome Trust Centre for Neuroimaging). EPI images were 1) aligned to the first image in each time series and used to estimate 6-parameter head movements for later use as nuisance regressors; 2) corrected for interleaved slice acquisition using the first slice as a reference; 3) co-registered to the mean functional image and to the individual anatomical volume; and 4) spatially normalized. The data were not smoothed.

I. B. General linear model. A general linear model was applied to the BOLD signal by convolving separate regressors for each of the 24 task states at the moment of response, and nuisance regressors for motion parameters and global signal, with a canonical hemodynamic response function. Data were visualized on the 6th generation 152 MNI images. All MRI analysis were carried out using SPM and customized MATLAB scripts. Normality of the data was confirmed by inspecting histograms of the beta values. Voxel locations are reported in MNI space using LPI coordinates.

II. REPRESENTATIONAL SIMILARITY SEARCHLIGHT ANALYSIS.

Representational similarity analysis (RSA) (4) assesses the correspondence between second-order isomorphisms associated with qualitatively different sources. In the present case, these sources are predictions of our neural network model and fMRI BOLD data. To conduct the searchlight analysis, first, a 27-element vector of BOLD signal activations was derived from each 3 × 3 × 3 voxel cube surrounding each voxel in the volume, for each of the 24 task states, separately for each subject. This yielded, for each participant, 24 vectors for each voxel, describing the pattern of activity in each local volume for each of the 24 states. Second, for each voxel, a separate representational dissimilarity matrix (RDM) was derived by computing the 1-

Spearman's rank correlation between all pairwise combinations of the 24 states. Third, the upper triangle of these RDMs was vectorized (ignoring elements along the diagonal), yielding a 276-unit vector for each voxel in the volume. Likewise, the upper triangle of the model-RDM was vectorized (ignoring elements along the diagonal), yielding a 276-element vector. Fourth, for each subject, the Spearman's rank correlation was computed between the 276-element model vector and each 276-element brain activation vector, yielding a correlation value for each voxel in the brain volume. Normality of the data was confirmed by inspecting histograms derived from the resulting correlation values. As we aimed to test the strong hypothesis that the model-RDM corresponds to MCC representations better than to the representations of other brain regions, as opposed to the weaker hypothesis that the model-RDM simply correlates with MCC representations, the correlation-values were z-transformed within-subjects; larger values therefore indicate brain areas that are relatively more correlated than other brain areas with the model-RDM.

III. PERMUTATION ANALYSIS.

For clustering purposes, voxels were thresholded at an uncorrected t-value corresponding to $p < .001$. To control for Type-1 error, a maximum cluster-level mass permutation analysis (5) was conducted by randomizing the elements of the predicted RDM 1000 times. For each permutation, 1) a searchlight analysis was conducted as described using the randomized RDM, 2) the t-values within each cluster were summed to determine the cluster-level mass for each cluster, and 3) the maximum cluster-level mass was retained. These 1000 values were then used to approximate the distribution of maximum cluster-level masses if the null hypothesis were true (5). A cluster associated with the predicted RDM was determined to be statistically significant if its cluster-level mass exceeded the 95% threshold of the distribution.

IV. MULTIDIMENSIONAL SCALING ANALYSIS.

For visualization purposes, nonmetric multidimensional scaling was applied to the context unit activation values, separately for each run of the model, using the MATLAB command:
yy=mdscale(1-cc,2,'start','random','criterion','metricsstres');

Data and code availability

Data and computer code will be made publicly available in an electronic repository.

Supplementary Text

I. BEHAVIORAL DATA. A 2-way within-subjects ANOVA on response times (RTs) with sequence type (4 levels) and sequence position (6 levels) as factors revealed a main effect of sequence position, $F(5,85) = 44.3$, $p < .001$, and an interaction between sequence type and sequence position, $F(15,255) = 2.6$, $p < .05$. There was no main effect of sequence type ($p > .05$), indicating that the sequences were equally difficult overall, although the interaction effect suggest that some steps of some sequences were more difficult than the same steps in other sequences.

II. MULTIDIMENSIONAL SCALING RESULTS. Multidimensional scaling (MDS) (6) of the context unit activations across the 24 states was conducted, revealing that the representations were characterized by 3 salient features (Fig. 1C). Each of these features was statistically robust across 100 runs of the model. To confirm the stability of these 3 predictions, we tested each of the 3 features independently. First, a t-test on the mean value across Spearman's rank correlations between the sequence position RDM (Fig. 5, Sequence Position) and the model-RDM (Fig. 1B), conducted separately for all 100 iterations of the model, confirmed that sequence position was a robust feature of the model representation, $t(99) = 33.53$, $p < .001$. Second, a t-test on the mean value across Spearman's rank correlations between the utensil RDM (Fig. 5, Utensil State) and the model-RDM (Fig. 1B), conducted separately for all 100 iterations of the model, confirmed that the model representations robustly distinguished between the utensil states and all of the other states, $t(99) = 57.36$, $p < .001$. Third, a t-test on the mean value across Spearman's rank correlations between the sequence identity RDM (Fig. 5, Sequence Identity) and the model-RDM (Fig. 1B), conducted separately for all 100 iterations of the model, confirmed that the model robustly distinguished between the different sequences, $t(99) = 123.5$, $p < 0.001$, $\text{mean}(r) = 0.81$, $\text{std}(r) = 0.66$.

Exploratory analyses.

I. SEQUENCE IDENTITY SEARCHLIGHT ANALYSIS. We applied the sequence identity RDM (Fig. 5, Sequence Identity) in a searchlight RSA following the same procedure used for the model-RDM RSA. This revealed a large, 1343-voxel cluster in the frontal pole centered on the right paracingulate gyrus in Brodmann area 32 and near Brodmann area 10 (Fig. S2, Table S2). The permutation analysis confirmed the statistical significance of the correlations between the searchlight-RDMs and the sequence identity RDM for voxels belonging to the cluster ($p < .05$). This result indicates that, although the medial-frontal cortex cluster is sensitive to sequence identity as discussed in the main text, the frontal pole exhibits greater sensitivity to sequence identity -- perhaps reflecting compliance with the task instructions to choose the sequences "as if flipping a coin". This interpretation is consistent with evidence implicating rostral prefrontal cortex in hierarchical control over sequential behavior (7, 8).

II. OTHER SEARCHLIGHT ANALYSES. We submitted RDMs that discriminated between the coffee vs. tea sequences (Fig. S3, left panel) and between sequences in which water was added first vs. sequences in which water was added second (Fig. S3, right panel) to separate searchlight RSAs according to the above procedure. In neither case did the results survive permutation analysis ($p > .05$).

Supplementary References

1. Schwartz F, et al. (1998) Naturalistic action impairment in closed head injury. *Neuropsychology* 12:13-28.
2. Shahnazian D, Holroyd CB (2018) Distributed representations of action sequences in anterior cingulate cortex: A recurrent neural network approach. *Psychon Bull Rev* 25:302-321.
3. Elman JL (1990) Finding structure in time. *Cogn Sci* 14:179-211.
4. Kriegeskorte N, Mur M, Bandettini P (2008) Representational similarity analysis - connecting the branches of systems neuroscience. *Front Syst Neurosci* 2:4.
5. Groppe DM, Urbach TP, Kutas M (2011) Mass univariate analysis of event-related brain potentials/fields I: A critical tutorial review. *Psychophysiology* 48:1711-1725.
6. Shepherd RN (1980) Multidimensional scaling, tree-fitting, and clustering. *Science* 210:390-398.
7. Desrochers TM, Chatham CH, Badre D (2015) The necessity of rostrolateral prefrontal cortex for higher-level sequential behavior. *Neuron* 87:1357-1368.
8. Mansouri FA, Koechlin E, Rosa MGP, Buckley MJ (2017) Managing competing goals - a key role for the frontopolar cortex. *Nat Rev Neurosci* 18:645-657.

Supplementary Figures

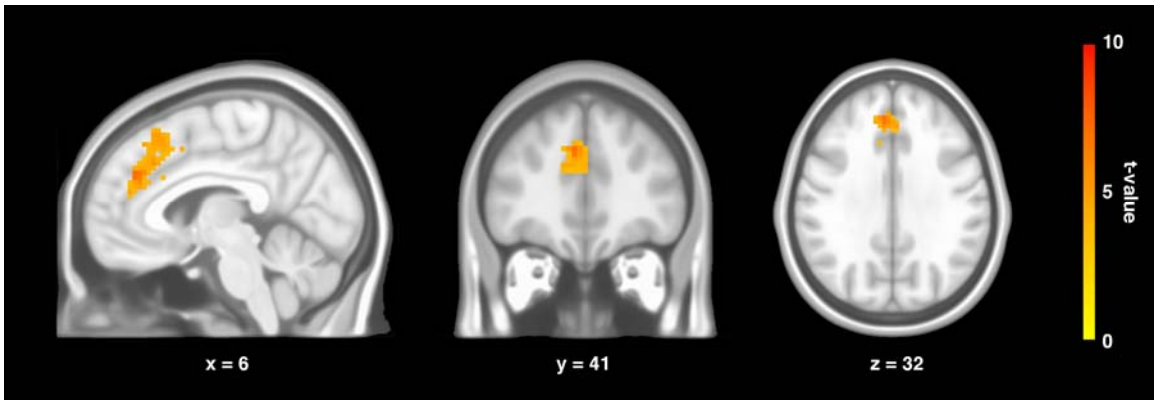

Figure S1. Representational similarity analysis results using the recurrent neural network representational dissimilarity matrix (RDM). Left panel: Sagittal view. Middle Panel: Coronal view. Right panel: Horizontal view. Color scale indicates t-test scores across subjects of the within-subject normalized Spearman correlation values between the model-RDM and the RDM for each searchlight volume. Only the cluster that survived the permutation analysis is shown. Views are centered on the peak value. Note that the stray voxels in this view are contiguous with the cluster in other slices. Note further that the left panel is identical to Figure 4A. Coordinates are indicated in MNI space and the underlay is ICBM MNI 152 6th generation.

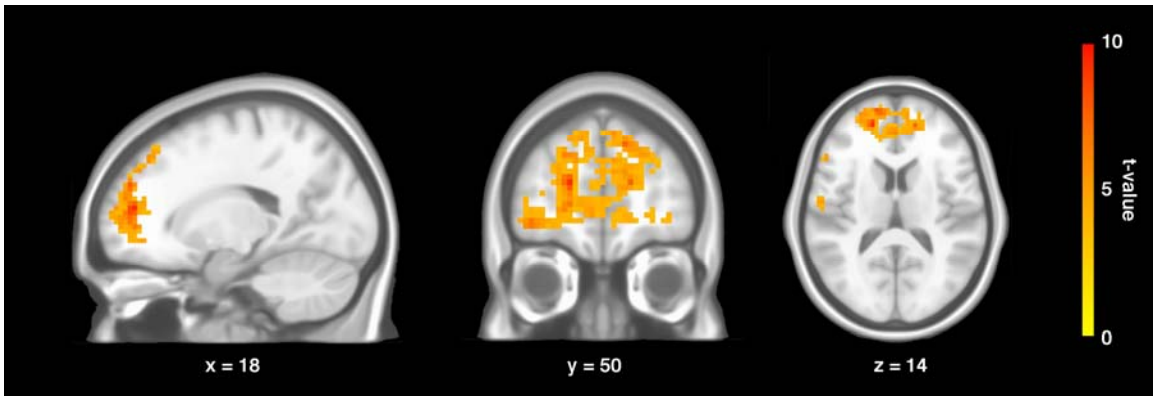

Figure S2. Primary cluster identified by the sequence identity searchlight analysis. The peak value is located in the right frontal pole in area Brodmann area 32. Left panel: Sagittal view. Middle Panel: Coronal view. Right panel: Horizontal view. Color scale indicates t-test scores across subjects of the within-subject normalized Spearman correlation values between the sequence identity RDM and the RDM for each searchlight volume. Views are centered on the peak t-value. Coordinates are indicated in MNI space and the underlay is ICBM MNI 152 6th generation.

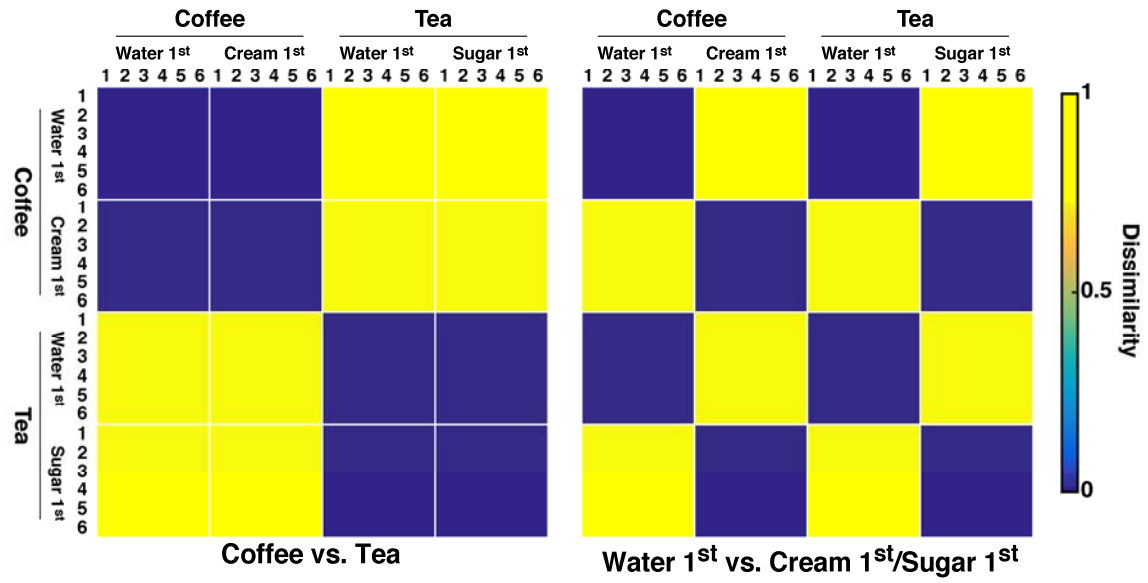

Figure S3. Representational dissimilarity matrices (RDMs) associated with exploratory analyses. Left: RDM discriminating the coffee sequences from the tea sequences. Right: RDM discriminating the sequences in which water was added first from the sequences in which water was added second. The 24 states along each axis correspond to the 6 actions associated with each of the 4 task sequences (coffee, water first; coffee, cream first; tea, water first; tea, sugar first; see Fig. 2). Blue indicates high similarity; yellow indicates low similarity. Units are arbitrary.

Supplementary Tables

Table S1. Representational similarity analysis cluster results using the recurrent neural network representational dissimilarity matrix.

Size	CMx	CMy	CMz	CM Location	CMBA	Px	Py	Pz	t	Peak Location	TBA
348	2	29	40	Right paracingulate gyrus	32	6	41	32	7.18	Right paracingulate gyrus	32
106	42	23	0	Right frontal operculum	47	48	20	2	6.39	Right frontal operculum cortex	45
69	46	19	25	Right inferior frontal gyrus Right pars opercularis	48	41	14	23	5.96	Right inferior frontal gyrus Right pars opercularis	48
60	-36	20	-2	Left insular cortex	47	-36	14	2	7.01	Left insular cortex	48
46	25	42	33	Right frontal pole	9	24	38	35	6.77	Right frontal pole	9
33	38	47	15	Right frontal pole	45	39	50	14	5.75	Right frontal pole	46

Size: Number of voxels in cluster. CMx, CMy, CMz: center of mass x, y and z MNI coordinates, respectively. CM Location: cortical areas associated with cluster center of mass. CMBA: Brodmann area associated with cluster center of mass. Px, Py, Pz: Peak t-value x, y and z MNI coordinates, respectively. t: cluster peak t-value. Peak Location: cortical areas associated with the cluster peak t-value. TBA: Brodmann area associated with the cluster peak t-value. Cortical areas are based on the Harvard-Oxford atlas using MRIcron. Cluster size is restricted to 30 voxels minimum. Note that only the largest cluster (348 voxels) survived the permutation analysis.

Table S2. Representational similarity analysis cluster results using the sequence identity representational dissimilarity matrix.

Size	CMx	CMy	CMz	CM Location	CMBA	Px	Py	Pz	T	Peak Location	TBA
1343	11.3	48.1	13.2	Right paracingulate gyrus	32	18	50	14	9.4	Right frontal pole	32
64	56.8	-18.2	1.6	Right inferior frontal gyrus Right pars opercularis	48	54	-31	5	7.5	Right inferior frontal gyrus Right pars triangularis	45
44	57.8	-7.6	21.8	Right precentral gyrus	6	60	-10	17	5.4	Right precentral gyrus	48

Size: Number of voxels in cluster. CMx, CMy, CMz: center of mass x, y and z MNI coordinates, respectively. CM Location: cortical areas associated with cluster center of mass. CMBA: Brodmann area associated with cluster center of mass. Px, Py, Pz: Peak t-value x, y and z MNI coordinates, respectively. t: cluster peak t-value. Peak Location: cortical areas associated with the cluster peak t-value. TBA: Brodmann area associated with the cluster peak t-value. Cortical areas are based on the Harvard-Oxford atlas using MRIcron. Cluster size is restricted to 30 voxels minimum. Note that only the largest cluster (1343 voxels) survived the permutation analysis.